

ANESTHESIOLOGY

Local Anesthetic Cardiac Toxicity Is Mediated by Cardiomyocyte Calcium Dynamics

Julia Plakhotnik, B.Sc., Libo Zhang, M.D., Ph.D.,
Marvin Estrada, R.V.T., John G. Coles, M.D.,
Per-Arne Lonnqvist, M.D., Ph.D., Jason T. Maynes, M.D., Ph.D.
Anesthesiology 2022; 137:687–703

EDITOR'S PERSPECTIVE

What We Already Know about This Topic

- Use of local anesthetics for perioperative pain control can be complicated by cardiotoxicity that may result in serious cardiac complications such as cardiac arrest.
- There is variability in cardiac toxicity of local anesthetics, with increased cardiotoxicity encountered with longer-acting (*e.g.*, bupivacaine) *versus* shorter-acting local anesthetics (*e.g.*, ropivacaine). The mechanism for this differing propensity to cardiac toxicity is not well understood.

What This Article Tells Us That Is New

- This study used human induced pluripotent stem cell–derived cardiomyocytes and found significantly altered cardiomyocyte calcium dynamics with bupivacaine but not ropivacaine. Calcium supplementation restored normal cardiomyocyte rhythm to bupivacaine-treated tissue. Calcium channel blockade selectively worsened bupivacaine cardiotoxicity.
- This study used a rat model (female) of cardiac toxicity and found that pretreatment with calcium improved survival of bupivacaine-treated rats and reduced survival of ropivacaine-treated rats.

Through peripheral neuron sodium channel (*e.g.*, Na_v1.7) blockade, local anesthetics provide regional anesthesia within a nerve distribution, reducing

ABSTRACT

Background: Long-lasting local anesthetic use for perioperative pain control is limited by possible cardiotoxicity (*e.g.*, arrhythmias and contractile depression), potentially leading to cardiac arrest. Off-target cardiac sodium channel blockade is considered the canonical mechanism behind cardiotoxicity; however, it does not fully explain the observed toxicity variability between anesthetics. The authors hypothesize that more cardiotoxic anesthetics (*e.g.*, bupivacaine) differentially perturb other important cardiomyocyte functions (*e.g.*, calcium dynamics), which may be exploited to mitigate drug toxicity.

Methods: The authors investigated the effects of clinically relevant concentrations of racemic bupivacaine, levobupivacaine, or ropivacaine on human stem cell–derived cardiomyocyte tissue function. Contractility, rhythm, electromechanical coupling, field potential profile, and intracellular calcium dynamics were quantified using multielectrode arrays and optical imaging. Calcium flux differences between bupivacaine and ropivacaine were probed with pharmacologic calcium supplementation or blockade. *In vitro* findings were correlated *in vivo* using an anesthetic cardiotoxicity rat model (females; *n* = 5 per group).

Results: Bupivacaine more severely dysregulated calcium dynamics than ropivacaine *in vitro* (*e.g.*, contraction calcium amplitude to $52 \pm 11\%$ and calcium-mediated repolarization duration to $122 \pm 7\%$ of ropivacaine effects, model estimate \pm standard error). Calcium supplementation improved tissue contractility and restored normal beating rhythm (to $101 \pm 6\%$, and $101 \pm 26\%$ of control, respectively) for bupivacaine-treated tissues, but not ropivacaine (*e.g.*, contractility at $80 \pm 6\%$ of control). Similarly, calcium pretreatment mitigated anesthetic-induced arrhythmias and cardiac depression in rats, improving animal survival for bupivacaine by 8.3 ± 2.4 min, but exacerbating ropivacaine adverse effects (reduced survival by 13.8 ± 3.4 min and time to first arrhythmia by 12.0 ± 2.9 min). Calcium channel blocker nifedipine coadministration with bupivacaine, but not ropivacaine, exacerbated cardiotoxicity, supporting the role of calcium flux in differentiating toxicity.

Conclusions: Our data illustrate differences in calcium dynamics between anesthetics and how calcium may mitigate bupivacaine cardiotoxicity. Moreover, our findings suggest that bupivacaine cardiotoxicity risk may be higher than for ropivacaine in a calcium deficiency context.

(ANESTHESIOLOGY 2022; 137:687–703)

perioperative systemic pain medication use. However, systemic anesthetic administration can occur *via* vascular uptake proximal to the anesthetized nerves, and/or inadvertent direct injection into blood vessels.¹ This results in

This article is featured in "This Month in Anesthesiology," page A1. Supplemental Digital Content is available for this article. Direct URL citations appear in the printed text and are available in both the HTML and PDF versions of this article. Links to the digital files are provided in the HTML text of this article on the Journal's Web site (www.anesthesiology.org). This article has a visual abstract available in the online version. Work presented in this article was presented at the Experimental Biology 2019 conference, Orlando, Florida, April 6 to 9, 2019, and at the American Society of Anesthesiologists 2021 Annual Meeting, San Diego, California, October 9 to 13, 2021.

Submitted for publication March 17, 2021. Accepted for publication September 14, 2022. Published online first on September 28, 2022.

Julia Plakhotnik, B.Sc.: Program in Molecular Medicine, The Hospital for Sick Children, Toronto, Canada; Department of Biochemistry, University of Toronto, Toronto, Canada.

Libo Zhang, M.D., Ph.D.: Program in Molecular Medicine, The Hospital for Sick Children, Toronto, Canada.

Marvin Estrada, R.V.T.: Laboratory Animal Services, The Hospital for Sick Children, Toronto, Canada.

John G. Coles, M.D.: Department of Cardiovascular Surgery, The Hospital for Sick Children, Toronto, Canada; Program in Translational Medicine, The Hospital for Sick Children, Toronto, Canada.

Per-Arne Lonnqvist, M.D., Ph.D.: Department of Physiology & Pharmacology, Karolinska Institute, Stockholm, Sweden; Paediatric Anesthesia & Intensive Care, Karolinska University Hospital, Stockholm, Sweden.

Jason T. Maynes, M.D., Ph.D.: Program in Molecular Medicine, The Hospital for Sick Children, Toronto, Canada; Department of Biochemistry, University of Toronto, Toronto, Canada; Department of Anesthesia and Pain Medicine, The Hospital for Sick Children, Toronto, Canada; Department of Anesthesiology and Pain Medicine, University of Toronto, Toronto, Canada.

Copyright © 2022, the American Society of Anesthesiologists. All Rights Reserved. Anesthesiology 2022; 137:687–703. DOI: 10.1097/ALN.0000000000004389

local anesthetic systemic toxicity estimated at 0.27 times per 1,000 nerve blocks.² Certain techniques, such as erector spinae plane block, may pose greater risks due to rapid systemic anesthetic absorption *via* the lymphatic.^{3,4} Toxicity typically presents with central nervous system and/or cardiovascular system symptoms, including seizures, arrhythmias, and contractile depression. The latter manifestations can lead to lethal cardiovascular collapse, observed in 5 to 10% of cases.² To minimize patient risk, the clinically used anesthetic doses are limited.⁵ Concern over racemic bupivacaine cardiotoxicity prompted development of less cardiotoxic long-acting anesthetics (e.g., ropivacaine, levobupivacaine). Although many anesthetics can cause cardiotoxicity, bupivacaine demonstrates a higher toxicity risk in human and animal studies and in clinical case reports.^{6–8} Current cardiotoxicity treatments are limited to specific cardiopulmonary support and intravenous lipid emulsion administration.^{1,5}

Preclinical investigations describe the Na_v1.5 cardiac sodium channel blockade as the canonical cardiotoxicity mechanism due to Na_v1.5 structural similarity to the intended target neuronal channels.⁷ However, human Na_v1.5 *in vitro* binding studies show only modest channel affinity differences between bupivacaine and ropivacaine.⁹ Besides Na_v1.5 binding, some anesthetics were shown to interact with cardiac L-type calcium channels and inhibit potassium repolarization currents.^{6,7,10,11} β -Adrenergic-mediated cAMP production blockade¹² and mitochondrial dysfunction, including acylcarnitine exchange inhibition and direct effects on electron transport,¹³ were also noted, albeit at concentrations well above clinical utility. Anesthetic dose inconsistencies and model variability (including described proteomic and physiologic differences between animal models and humans) make it challenging to translate observed discrepancies in cardiotoxicity mechanisms into clinical utility.⁷ This issue applies more broadly to many pharmaceuticals demonstrating unexpected postmarket cardiotoxicity.¹⁴

To assess cardiotoxicity risk and improve clinical translation, human induced pluripotent stem cell-derived cardiomyocytes can be used to supplement animal data. We and others have shown that these cells provide a cardiomyocyte model that exhibits a human physiologic ion channel and contractile protein profile, yielding expected responses to cardiotropic drugs.^{14–16} To identify potential toxicity risks, we sought to elucidate and contrast the mechanisms involved in local anesthetic cardiotoxicity using stem cell-derived cardiomyocyte tissues. We hypothesized that accompanying canonical Na_v1.5 blockade, bupivacaine and ropivacaine divergently perturb additional key cardiomyocyte processes, such as calcium dynamics, consistent with observed *in vivo* cardiotoxicity differences. These mechanisms could potentially be exploited for context-specific toxicity prevention. Therefore, we evaluated bupivacaine and ropivacaine impact on contractility and

arrhythmogenesis in human-based tissues and a rat model, contrasting calcium supplementation effects. To further test the role of calcium flux in anesthetic-specific cardiotoxicity, we compared the effects of calcium supplementation or calcium channel blockade on cardiomyocyte function and intracellular calcium dynamics.

Materials and Methods

Tissue Culture

Human induced pluripotent stem cell-derived cardiomyocytes (iCell Cardiomyocytes,² Cellular Dynamics International, USA) were thawed using Plating Medium (Cellular Dynamics) and cultured per manufacturer instructions in Maintenance Medium (Cellular Dynamics). Culture media contain galactose instead of glucose to encourage energy production through oxidative phosphorylation, promoting cardiomyocyte maturation. Microplates were coated with a mixture of gelatin (0.25 mg/ml), fibronectin (10 μ g/ml), and laminin (5 μ g/ml) before cell seeding.

Multielectrode Array Recordings of Tissue Function

Human induced pluripotent stem cell-derived cardiomyocytes were seeded onto 48-well Cardio ECR E-plates (Acea Biosciences, USA) at 45,000 cells/well. Cell contractility (impedance) and electrical activity (field potential) were simultaneously monitored using the xCELLigence RTCA Cardio ECR (Acea Biosciences). Beat interval deviation was calculated as the median absolute deviation of beat-to-beat intervals,¹⁷ corrected for beating rate as per Monfredi *et al.*¹⁸ After monolayer formation and stable beating (5 days), tissues were further matured by electrical stimulation (1, 1.5, and 2 Hz consecutively for 5 days each), then allowed rest to stabilize beating (at least 1 day) before drug treatment. Recordings (1-min duration, at 10- to 20-min intervals) were captured at baseline before drug treatment/cotreatment, then starting again at 5 h after drug treatment to minimize the disturbance of handling the tissues. For dose-response experiments, bupivacaine or ropivacaine were used at 0.1 to 9 μ g/ml, or levobupivacaine at 0.1 to 6 μ g/ml, corresponding to 0.3 to 27.7 μ M bupivacaine, 0.3 to 28.9 μ M ropivacaine, or 0.3 to 18.5 μ M levobupivacaine; $n = 6$ to 9 measurements per three to four tissues per concentration. For calcium cotreatment experiments, bupivacaine or ropivacaine were used at 6 μ g/ml (18.5 and 19.3 μ M, respectively); $n = 6$ to 12 measurements per two to four tissues per concentration. For treatment causing beating arrest (all tissues at 9 μ g/ml bupivacaine), the amplitude of either the impedance or the field potential noise signal was used in amplitude analysis to obtain a baseline value, but excluded from analysis of other metrics.

Functional Tissue Analysis Using Optical Imaging

Induced pluripotent stem cell–derived cardiomyocytes were seeded at 20,000 cells/well on microplates coated with a silicone polymer (Young's modulus 5 kPa),¹⁹ mimicking healthy myocardial stiffness,²⁰ and cultured for 4 weeks to allow tissue formation and maturation. Maturation of the calcium-handling sarcoplasmic reticulum structure was verified by immunostaining sample tissues for the sarcoendoplasmic reticulum calcium ATPase (Supplemental Figure S1, <http://links.lww.com/ALN/C936>).^{21,22} Videos were captured for 12 s using a Zeiss Axio Observer 7 epifluorescence microscope equipped with automated stage control (allowing multipoint acquisition) and environmental darkroom chamber (kept at 37°C, 5% CO₂). For label-free functional assessment, baseline videos were captured at 60 frames per second in brightfield immediately before drug or cotreatment addition, then again 5 h after treatment. Bupivacaine or ropivacaine were used at 2, 4, or 6 µg/ml, corresponding to 6.1, 12.3, or 18.5 µM bupivacaine or 6.4, 12.9, or 19.3 µM ropivacaine; n = 2 to 6 measurements per three to four tissues per group. Cotreatment with 6 µg/ml bupivacaine and 50 nM nifedipine caused beating arrest (all three tissues), which were excluded from further analysis. For assessment of intracellular calcium dynamics, tissues were loaded with FLIPR5 intracellular calcium dye (Molecular Devices, USA, diluted 1:3 in Cellular Dynamics Maintenance Medium) 5 h after treatment. Dye addition was staggered to match exposure time before imaging, with total dye incubation time of 45 min per well. Videos were captured at 45 frames per second in a fully automated fashion, ensuring equal dye incubation and light source exposure settings per sample per experiment (488 nm excitation, 525 nm emission). Bupivacaine or ropivacaine were used at both 2 and 6 µg/ml, and at 6 µg/ml for calcium cotreatment experiments; n = 76 to 132 measurements per three to four tissues per group. For nifedipine cotreatment calcium dynamics, because 6 µg/ml bupivacaine caused arrest, 4 µg/ml anesthetic dose was used; n = 10 to 36 measurements per four tissues per group. Videos were processed using fully automated, custom, laboratory-developed R and Python software, based on published algorithms to track tissue motion²³ and calcium flux^{24,25} during beating cycles. FLIPR5 fluorescence was normalized to minimum fluorescence for each field of view (*i.e.*, relaxation baseline), representing relative intracellular calcium intensity during beating (F/F_0).

In Vivo Rat Model

Following published anesthetic cardiotoxicity models,²⁶ female Sprague-Dawley rats (300 to 400 g, purchased from Lab Animal Services, Hospital for Sick Children, Toronto) were housed two per cage in a controlled environment (12 h light-dark cycle), with free access to food and water. Experiments were performed at the same time of day during daylight hours. Animals were anesthetized (2% isoflurane),

intubated *via* tracheostomy, and mechanically ventilated (10 ml/kg tidal volume at 65 breaths/min). Rectal temperature was maintained 36.5° to 37.5°C using underbody warming. Animals were randomized to two pretreatment groups per cage (10 mg/kg CaCl₂ in saline *vs.* saline), with the experimenter blinded to pretreatment, and assessed in sequential order. The pretreatment regimen was intravenously infused (24-gauge tail vein catheter) over 5 min, then after 5 min rest, anesthetics (1% bupivacaine or ropivacaine in saline) were infused until asystole (2 mg·kg⁻¹·min⁻¹, five animals per group). Blood oxygen saturation, arterial blood pressure (*via* 24-gauge catheter in the carotid artery) and 3-lead ECG were recorded every 2.5 to 5 min (Mindray PM9000Vet) after beginning of anesthetic infusion; n = 9 to 16 measurements per five animals per group. Arterial blood (0.3 ml) was sampled for blood gas and electrolytes once before pretreatment and once postasystole (i-STAT1 using CG8+ cartridges; Abbott, USA), and was not sampled in two rats due to an insufficient amount of blood obtained (excluded from analysis). Primary outcomes were the time to asystole (defined as absence of ECG activity for 10 s) and the time to first arrhythmia (defined as identifiable early or delayed afterdepolarizations, or irregular RR intervals lasting at least 2 s on the ECG, that were accompanied by irregular systolic intervals on the arterial blood pressure trace). Animals were terminated by isoflurane overdose.

Drugs

All drugs were purchased from Alfa Aesar (USA). Racemic bupivacaine, S-bupivacaine (levobupivacaine), and S-ropivacaine were used in all experiments, as specified.

Data Analysis and Statistics

Due to replicate measures and multiple predictor study designs, data were analyzed using mixed-effects linear (in the case of normally distributed data) or generalized linear (in the case of nonnormally distributed data) multiple regression in R version 4.1.1, including predictor (main effects) interaction terms and random error accounting for sample replication (as stated earlier and in figure legends). Anesthetic × cotreatment were the main effects in the *in vitro* studies; anesthetic × pretreatment × time were the main effects in the rat model, paired by cage to account for variation due to animal litters and day of procedure. Time-course rat hemodynamic parameters were fit *via* third-order polynomial with respect to time, with baseline pretreatment values as a covariate term. For *in vitro* tissue studies, data were normalized to baseline measurements per sample, then expressed as ratios of time-matched vehicle control tissues. All datapoints are shown in the figures, where possible, otherwise provided in the supplementary figures (<http://links.lww.com/ALN/C936>). No statistical power calculation was conducted before the study; sample size was based on previous experience. Data distribution was evaluated *via* Cullen and Fray plots (R package “fitdistrplus”). Models were built

using the R packages “lme4” (equal group variance) and “glmmTMB” (nonequal group variance) using restricted maximum likelihood. Model assumptions were tested by examining residual plots for normal distribution and homoscedasticity, and fit was evaluated by examining model estimates and errors in relation to input data. Results are presented as marginal model means and standard error, estimated using the “emmeans” R package to account for any sample size imbalance between groups. *Post hoc* comparisons were performed in “emmeans” *via* two-sided Welch’s *t* tests, and expressed as ratios to vehicle control group, then further comparisons made where shown in the figures. The 95% CIs and *P* values were adjusted for multiple comparisons (Dunnnett when comparing to a control group; Tukey otherwise); significance was designated at $P < 0.05$ ($P < 0.1$ for interactions). Bootstrap CIs were generated using non-parametric bootstrap (R package “Hmisc”) with 1,000 resamples. In response to peer review, dose–response data were added—curves were generated by fitting a Hill function (variable slope, R package “drc”); estimated EC50 values are reported with standard error.

Study Approval

All experiments were approved by the Institutional Animal Care and Use Committee of the Hospital for Sick Children (Toronto, Canada) and performed in accordance with national, institutional, and ARRIVE 2.0 guidelines for animal care.

Results

Racemic Bupivacaine Inhibits Human Cardiomyocyte Tissue Contractility and Perturbs Integrated Ion Channel Activity

To differentiate how bupivacaine or ropivacaine may alter cardiomyocyte function and to define a toxicity threshold within typical clinically relevant serum concentrations (0.1 to 9 $\mu\text{g/ml}$),^{27–31} we evaluated drug effects on functional beating monolayers of human induced pluripotent stem cell–derived cardiomyocytes. For comparison with racemic bupivacaine, we additionally investigated levobupivacaine, the pure bupivacaine *S*-enantiomer with a lower clinical cardiotoxicity risk.^{6,8} Using a combined impedance and field potential multielectrode array, we measured tissue physical contraction (*via* tissue impedance) and captured changes to electric field potential, allowing for simultaneous evaluation of contraction, beat rate and rhythm, electromechanical coupling, and action potential profile³² (figs. 1A and 2A). At 2 $\mu\text{g/ml}$ dose and below, consistent with previous *in vivo* data,^{27,29,31} we did not observe any significant changes from baseline to tissue physical contraction or beating rhythm, for any anesthetic. Our only observation was a small decrease in beating rate at 2 $\mu\text{g/ml}$ bupivacaine (fig. 1).

Starting at 3 $\mu\text{g/ml}$, bupivacaine more strongly inhibited contractile amplitude, beating rate (beats/min EC50 7.3 ± 0.5 μM for bupivacaine and 11.7 ± 0.8 μM for ropivacaine), and induced dysrhythmic beating (beat interval deviation EC50 6.8 ± 0.9 μM for bupivacaine and 12.5 ± 3.6 μM for ropivacaine; fig. 1). The difference in contractile depression increased with higher doses (fig. 1B). At 6 $\mu\text{g/ml}$, bupivacaine more severely depressed contractile amplitude (to $55 \pm 4\%$ of control, $P < 0.001$, and $73 \pm 6\%$ of ropivacaine effect, $P = 0.001$), and induced 9.0 ± 5.1 -fold higher beat interval deviation (dysrhythmia) than ropivacaine ($P < 0.001$). At 9 $\mu\text{g/ml}$, bupivacaine caused complete beating arrest of all tissues (noise-only impedance and field potential signal); however, ropivacaine effects were comparable to those at 6 $\mu\text{g/ml}$. Levobupivacaine effects were most similar to ropivacaine overall (fig. 1B; *e.g.*, beat interval deviation $P = 0.999$). Together, these results are consistent with increased bupivacaine cardiac contractile depression and arrhythmias observed clinically.^{2,6} For corroboration, we quantified the effects of bupivacaine and ropivacaine on stem cell–derived cardiomyocyte tissues cultured on soft substrates (5 kPa), to mimic physiologic myocardial stiffness.^{19,20} Similarly, we observed reductions in contractility measures (tissue displacement amplitude and contractile velocity) for both drugs above the subtoxic 2 $\mu\text{g/ml}$ concentration (Supplemental Figure S2, <http://links.lww.com/ALN/C936>). The magnitude of these adverse effects was significantly larger for bupivacaine than for ropivacaine at both 4 and 6 $\mu\text{g/ml}$ (*e.g.*, bupivacaine decreased tissue contraction–phase velocity to $47 \pm 8\%$ of ropivacaine effect at 6 $\mu\text{g/ml}$ anesthetic, $P < 0.001$).

To determine anesthetic effects on cardiomyocyte electromechanical coupling, we measured the coordinated timing of electrical excitation and cell contraction (excitation–contraction coupling time), *via* simultaneous capture of tissue impedance (physical contraction) and field potential (membrane potential) recordings (fig. 2A). All drugs prolonged the excitation–contraction coupling time at 6 $\mu\text{g/ml}$ (bupivacaine to $144 \pm 5\%$, ropivacaine to $125 \pm 4\%$, and levobupivacaine to $128 \pm 4\%$ of control, $P < 0.001$ for all), indicative of impaired coordination between membrane depolarization and physical contraction. However, we observed markedly different field potential profiles between the anesthetics, as a measure of integrated channel activity^{33,34} (fig. 2). All drugs reduced total sodium spike amplitude, indicative of expected sodium current ($\text{Na}_v1.5$) inhibition during depolarization, but bupivacaine decreased sodium spike amplitude more than ropivacaine (EC50 7.5 ± 0.4 *vs.* 25.2 ± 5.1 μM ; decrease to $13 \pm 2\%$ of control and $22 \pm 4\%$ of ropivacaine effect at 6 $\mu\text{g/ml}$, $P < 0.001$ for both). Interestingly, bupivacaine-treated tissues showed a more pronounced delay in early-phase repolarization compared to ropivacaine-treated tissues, indicative of greater perturbation of calcium currents (EC50 8.2 ± 0.5 *vs.* 15.9 ± 3.4 μM ; increase to $131 \pm 5\%$ of

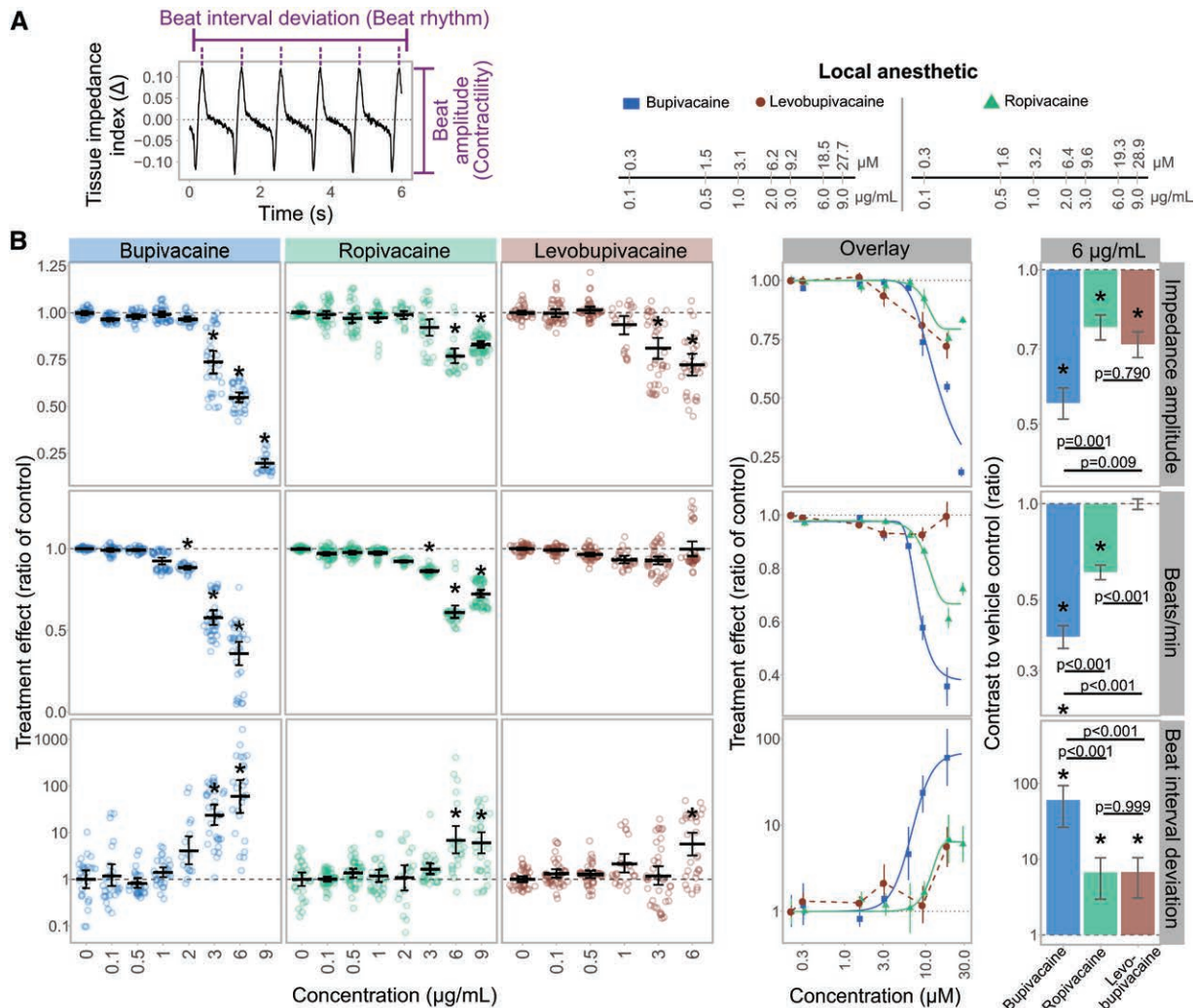


Fig. 1. Bupivacaine depresses cardiomyocyte tissue contractility and induces arrhythmias more potently than ropivacaine and levobupivacaine. Human induced pluripotent stem cell–derived cardiomyocyte tissues were treated with typical clinically relevant concentrations (0.1 to 9 $\mu\text{g/mL}$ equaling 0.3 to 28.9 μM) of bupivacaine, ropivacaine, or levobupivacaine. Functional measurements were obtained using a multi-electrode array. (A) Example baseline multi-electrode array tracing. Tissue contractility was evaluated as the beat amplitude of tissue impedance; beating rhythm as median absolute deviation of beat-to-beat intervals, corrected for beating rate. (B) Quantification of drug-induced changes to contractile amplitude, beating rate, and beating irregularity shows increased effects of bupivacaine. Data are mean and 95% bootstrap CI. Bars (right) are mixed-effects model estimates and standard error comparing each anesthetic at the toxic 6 $\mu\text{g/mL}$ dose. Hill curves (overlay) were fit where possible (parameter $P < 0.05$; solid lines); dashed lines plotted otherwise. $n = 4$ tissues per concentration (3 for 2 $\mu\text{g/mL}$ groups); 6 to 9 measurements per tissue at 5 h after treatment. * $P < 0.05$ treatment versus time-matched vehicle controls (0 $\mu\text{g/mL}$); additional comparisons stated on the plot (multiplicity-adjusted *post hoc* Welch's *t* tests of mixed-effects model estimates).

control and $122 \pm 7\%$ of ropivacaine effect at 6 $\mu\text{g/mL}$, $P < 0.001$ for both). Comparable to ropivacaine, we did not observe a change in early-phase repolarization with levobupivacaine (fig. 2B). Last, we did not detect a measurable difference between the anesthetics in late-phase repolarization time, corresponding to potassium-mediated membrane repolarization ($P > 0.16$ at 6 $\mu\text{g/mL}$ for all drugs). In general, levobupivacaine showed contractility, rhythm, and field potential effects most similar to ropivacaine (figs. 1 and 2),

consistent with previous work and clinical toxicity observations.^{2,8} Thus, we focused on comparing bupivacaine to ropivacaine in the following experiments.

Calcium Supplementation Rescues Bupivacaine-Mediated Contractile Dysfunction

Calcium supplementation can be used to improve cardiac inotropy; however, excess intracellular calcium can lead to arrhythmias.^{22,35} Because bupivacaine was

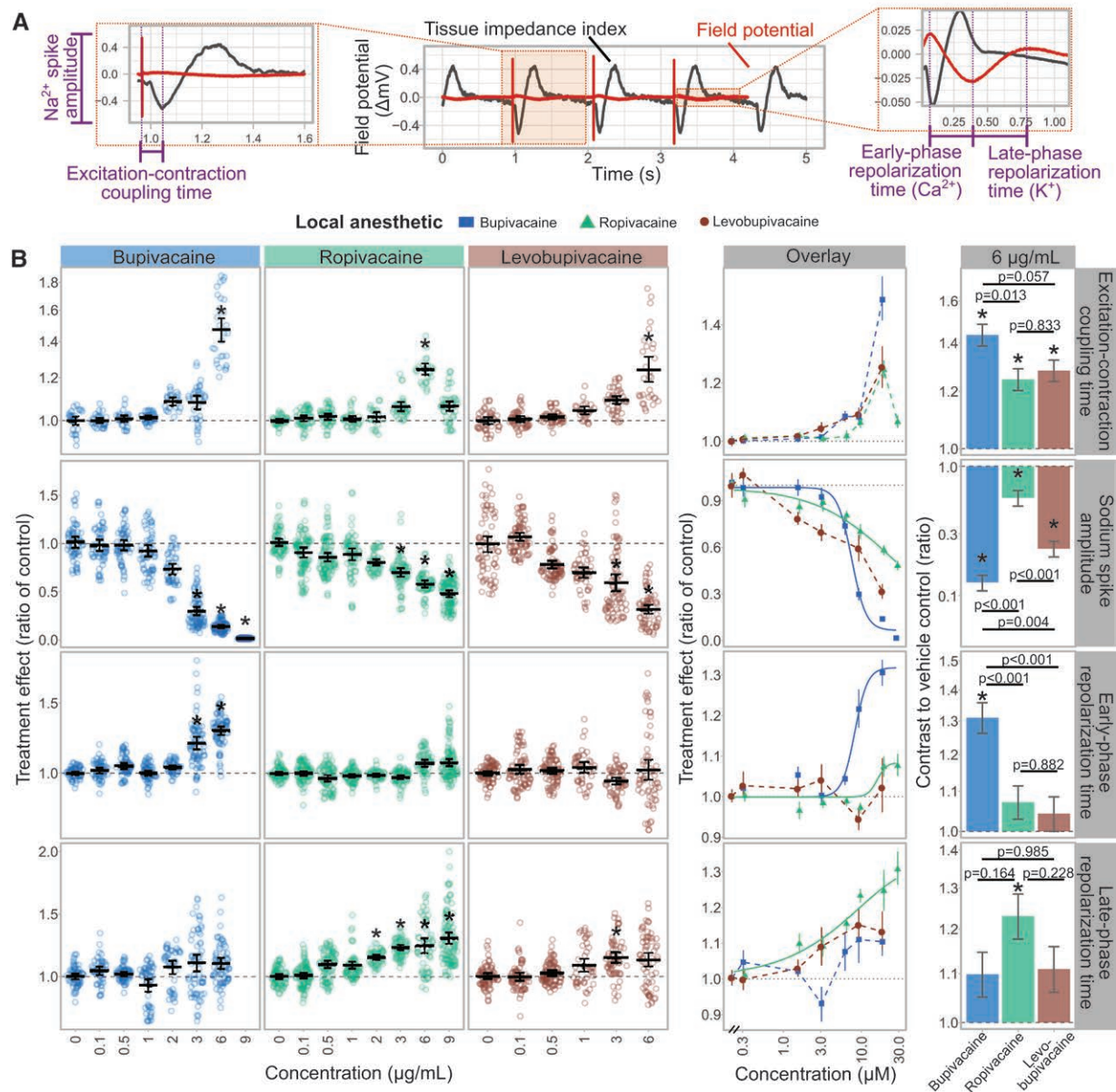


Fig. 2. Bupivacaine more potently perturbs cardiomyocyte field potentials. Human induced pluripotent stem cell-derived cardiomyocyte tissues were treated with typical clinically relevant concentrations (0.1 to 9 µg/ml equaling 0.3 to 28.9 µM) of bupivacaine, ropivacaine, or levobupivacaine. Functional measurements were obtained using a multielectrode array. (A) Example trace illustrating the simultaneous collection of cellular field potentials and tissue contractility (impedance), allowing for quantification of sodium spike amplitude, early and late repolarization, and the excitation-contraction coupling time. (B) Quantification of treatment effects shows decreased sodium spike amplitude and altered field potential profiles. Data are mean and 95% bootstrap CI. Bars (right) are mixed-effects model estimates and SE comparing each anesthetic at the toxic 6 µg/ml dose. Hill curves (overlay) were fit to bupivacaine and ropivacaine data where possible (parameter $P < 0.05$; solid lines); dashed lines plotted otherwise. $n = 4$ tissues per concentration (3 for 2 µg/ml groups); 12 to 18 measurements per tissue (6 to 9 for excitation-contraction coupling time) at 5 h after treatment. * $P < 0.05$ treatment versus time-matched vehicle controls (0 µg/ml); additional comparisons stated on the plot (multiplicity-adjusted *post hoc* Welch's *t* tests of mixed-effects model estimates).

previously noted to antagonize L-type calcium channels,³⁶ which is supported by our data, we tested the ability of moderate calcium supplementation to

attenuate anesthetic toxicity at a dose showing quantifiable arrhythmias and contractile depression for both drugs (6 µg/ml anesthetic). Coadministration of

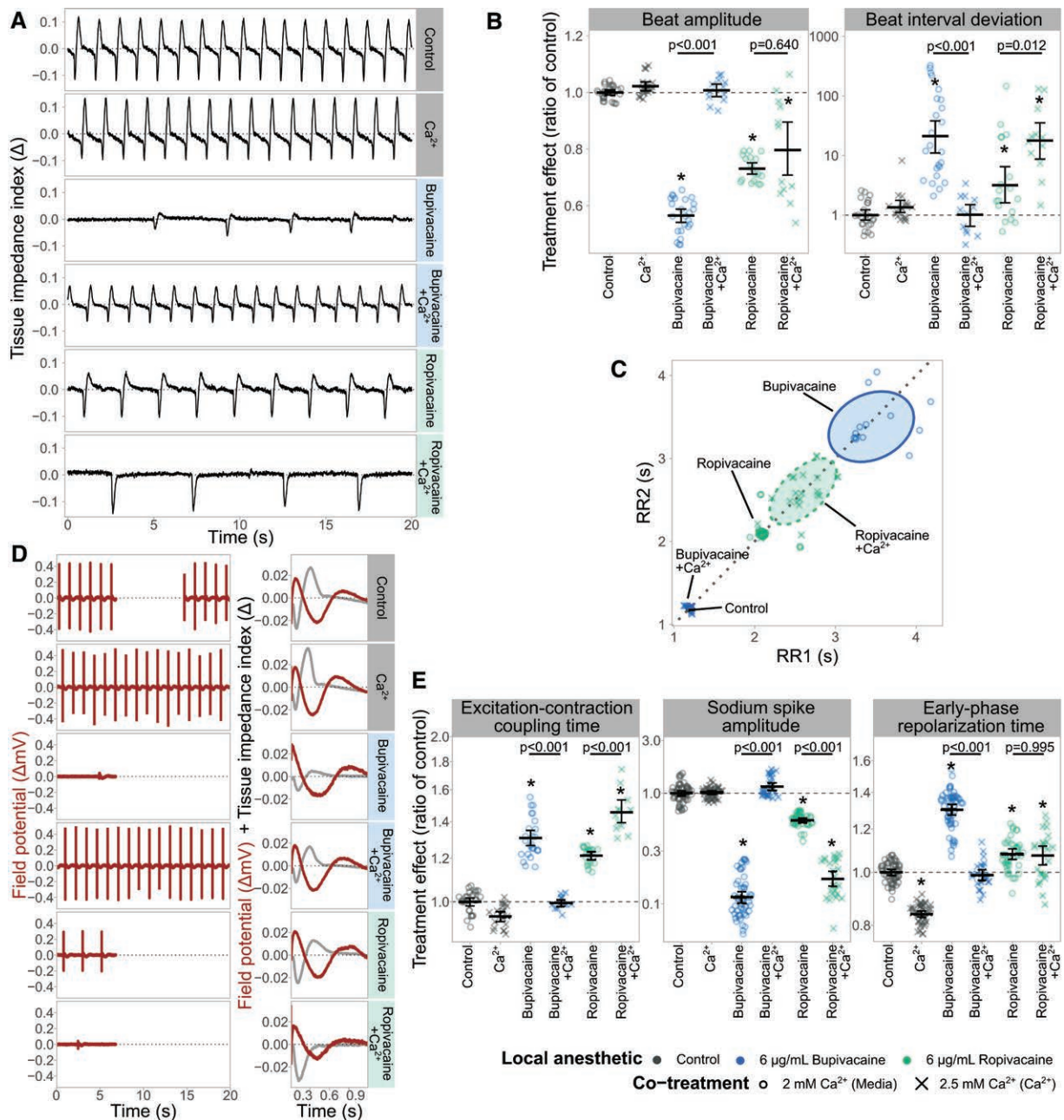


Fig. 3. Bupivacaine adverse effects on cardiomyocyte contractility, beating rhythm, and field potential profile are rescued by exogenous calcium. Induced pluripotent stem cell–derived cardiomyocyte tissues were treated with 6 $\mu\text{g/mL}$ bupivacaine or ropivacaine, where quantifiable arrhythmias were previously observed for both drugs. Calcium (final concentrations of 2.5 mM CaCl_2 vs. 2 mM in culture medium) was supplemented concurrently with drug treatment (cotreatment) after baseline recordings in a subset of tissues. (A) Representative beating traces illustrating a decreased contractile amplitude and increased beating irregularity of bupivacaine-treated tissues compared to ropivacaine. Adverse effects of bupivacaine were mitigated by treatment with exogenous calcium, which exacerbated ropivacaine dysrhythmia, as quantified in **B**. (C) Poincaré plot of subsequent beat-to-beat intervals (RR1 and RR2) showing representative beat interval deviation between treatment groups as 90% confidence ellipse around the points. Larger ellipse indicates higher beating irregularity. (D) Representative field potential beating traces (left) and beat-averaged repolarization with impedance waveforms (right). (E) Quantification of treatment effects shows that the decreased sodium spike amplitude and altered field potential profile was restored to baseline by calcium supplementation in bupivacaine-treated, but not ropivacaine-treated tissues. The differential effect of calcium was supported by anesthetic and cotreatment interaction $P < 0.001$ for all metrics. Data are mean and 95% bootstrap CI. $n = 4$ tissues for control, bupivacaine groups (3 for calcium, ropivacaine; 2 otherwise); 6 measurements per tissue (12 for sodium amplitude and repolarization time) at 5-h treatment time frame. * $P < 0.05$ treatment versus time-matched vehicle control; additional comparisons stated on the plot (multiplicity-adjusted *post hoc* Welch's *t* tests of mixed-effects model estimates).

calcium chloride (final concentration 2.5 mM Ca^{2+} vs. 2 mM Ca^{2+} in media-only controls) corrected bupivacaine-induced changes to impedance amplitude (to $101 \pm 6\%$ of control, $P = 0.999$) and beating interval deviation (to 1.0 ± 0.3 -fold of control, $P = 0.999$), indicating mitigation of contractile depression and arrhythmia (fig. 3 and Supplemental Figure S3, <http://links.lww.com/ALN/C936>). Conversely, cotreatment of ropivacaine tissues did not alter impedance amplitude ($80 \pm 6\%$ of control, $P = 0.012$, and $109 \pm 10\%$ of ropivacaine, $P = 0.640$), and exacerbated beat interval deviation (to 17.8 ± 7.3 -fold of control, $P < 0.001$, and 4.9 ± 2.7 -fold of ropivacaine-only tissues, $P = 0.012$), indicating increased arrhythmic beating (fig. 3, A to C). Calcium supplementation corrected the delay in excitation-contraction coupling time caused by bupivacaine but worsened the change in ropivacaine-treated tissues (fig. 3E). Similar changes were observed in sodium spike

amplitude and early-phase repolarization time, reflecting the divergent effects of the two anesthetics on cellular field potentials, and the ability of exogenous calcium to correct bupivacaine adverse alterations.

Disruption of Intracellular Calcium Dynamics by Bupivacaine Is Partially Recovered by Calcium Supplementation

Given the observed differences in calcium currents and the effects of calcium supplementation between the two anesthetics, we further investigated sarcolemmal calcium dynamics of anesthetic-treated stem cell-derived cardiomyocyte tissues *via* intracellular calcium imaging^{24,25} (fig. 4A). We did not observe any significant differences between the two drugs at the subtoxic 2 $\mu\text{g}/\text{ml}$ concentration (Supplemental Figure S4, <http://links.lww.com/ALN/C936>).

However, at 6 $\mu\text{g}/\text{ml}$, bupivacaine more significantly affected all phases of calcium flux in the beating cycle than

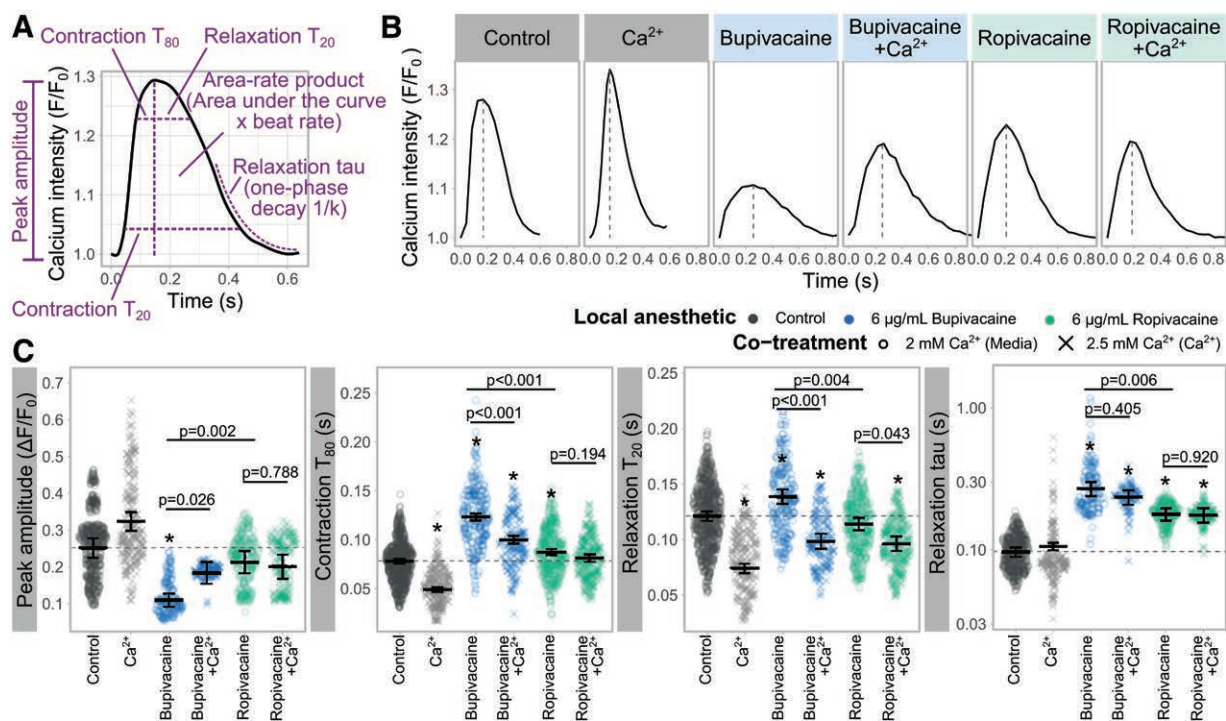


Fig. 4. Disruption of cardiomyocyte calcium dynamics by bupivacaine is partially mitigated by exogenous calcium. Induced pluripotent stem cell-derived cardiomyocyte tissues were treated with 6 $\mu\text{g}/\text{ml}$ bupivacaine or ropivacaine, and a subset concurrently supplemented with calcium chloride (final concentration 2.5 mM vs. 2 mM in culturing medium). (A) Example trace of intracellular calcium dynamics captured from automated video microscopy using FLIPR5 (calcium sensitive) fluorescent dye, including contraction and relaxation beating phases. (B) Representative calcium fluorescence intensity traces (one beat) illustrating significant perturbation of intracellular calcium dynamics by bupivacaine (and to a greater extent than ropivacaine), quantified in C. Both contraction (calcium release) and relaxation (calcium reuptake into the sarcoplasm) were affected more severely by bupivacaine, with partial mitigation of these effects by calcium supplementation. Data are mean with 95% bootstrap CI. $n = 4$ tissues for control, ropivacaine groups (2 for calcium; 3 otherwise); 76 to 132 measurements per tissue at 5 h after treatment, * $P < 0.05$ treatment versus time-matched vehicle control; additional comparisons stated on the plot (multiplicity-adjusted *post hoc* Welch's *t* tests of mixed-effects model estimates). Anesthetic and cotreatment peak amplitude interaction $P = 0.071$; contraction T_{80} $P = 0.061$; relaxation T_{20} $P = 0.131$; relaxation tau $P = 0.587$.

ropivacaine. Bupivacaine decreased peak calcium wave amplitude (to $44 \pm 9\%$ of control, $P < 0.001$, and $52 \pm 11\%$ of ropivacaine effect, $P = 0.002$) and prolonged contraction T_{80} (time to reach 80% peak calcium intensity), indicating decreased peak cytosolic calcium and slowed release from the sarcoplasmic reticulum during contraction (fig. 4). Furthermore, bupivacaine prolonged relaxation T_{20} (time to reach 20% of calcium decay) and increased the relaxation time constant tau (to 2.8 ± 0.4 -fold of control, $P < 0.001$, and 1.5 ± 0.2 -fold of ropivacaine effect, $P = 0.006$), indicating slower kinetics in both early and late phases of sarcoplasmic calcium reuptake during relaxation (fig. 4). Similar results were observed at $4 \mu\text{g/ml}$ in subsequent experiments (fig. 5C).

We compared the ability of calcium supplementation to attenuate the adverse changes to calcium dynamics observed at the toxic $6 \mu\text{g/ml}$ anesthetic dose. The effects of calcium supplementation on sarcoplasmic reuptake did not differ between the two anesthetics (fig. 4C), but calcium effects on contraction dynamics (*i.e.*, sarcoplasmic release) were distinct. In bupivacaine-treated tissues, calcium cotreatment increased peak calcium wave amplitude ($P = 0.026$ *vs.* bupivacaine-only), and reduced contraction T_{80} ($P < 0.001$ *vs.* bupivacaine-only), indicating increased cytosolic calcium and speed of release from the sarcoplasm, partially mitigating the negative bupivacaine effects (fig. 4). Conversely, calcium did not affect peak wave amplitude ($P = 0.788$) or contraction T_{80} ($P = 0.194$) in ropivacaine-treated tissues (fig. 4). These findings mirror the calcium supplementation effects on contraction amplitude, where calcium mitigated the bupivacaine contractile depression, but showed no effects in ropivacaine-treated tissues (fig. 3).

Overall, we found that both anesthetics lacked significant effects on cardiomyocyte function at subtoxic doses. However, above the toxic threshold, bupivacaine perturbed contractility, was more arrhythmogenic, and adversely affected calcium dynamics to a larger degree than ropivacaine. Calcium cotreatment mitigated the bupivacaine-induced changes, but exacerbated the negative effects of ropivacaine, highlighting the role of altered calcium flux in the different cardiotoxicity mechanisms between the two anesthetics (Supplemental Figure S5, <http://links.lww.com/ALN/C936>).

Exogenous Calcium Attenuates Bupivacaine Cardiotoxicity *In Vivo*

To validate our human induced pluripotent stem cell-derived cardiomyocyte tissue findings, we tested anesthetic effects in an *in vivo* rat model of anesthetic cardiotoxicity.²⁶ Equal doses of bupivacaine or ropivacaine were continuously infused (intravenous) to gradually reach toxic serum concentrations, with continuous invasive arterial pressure

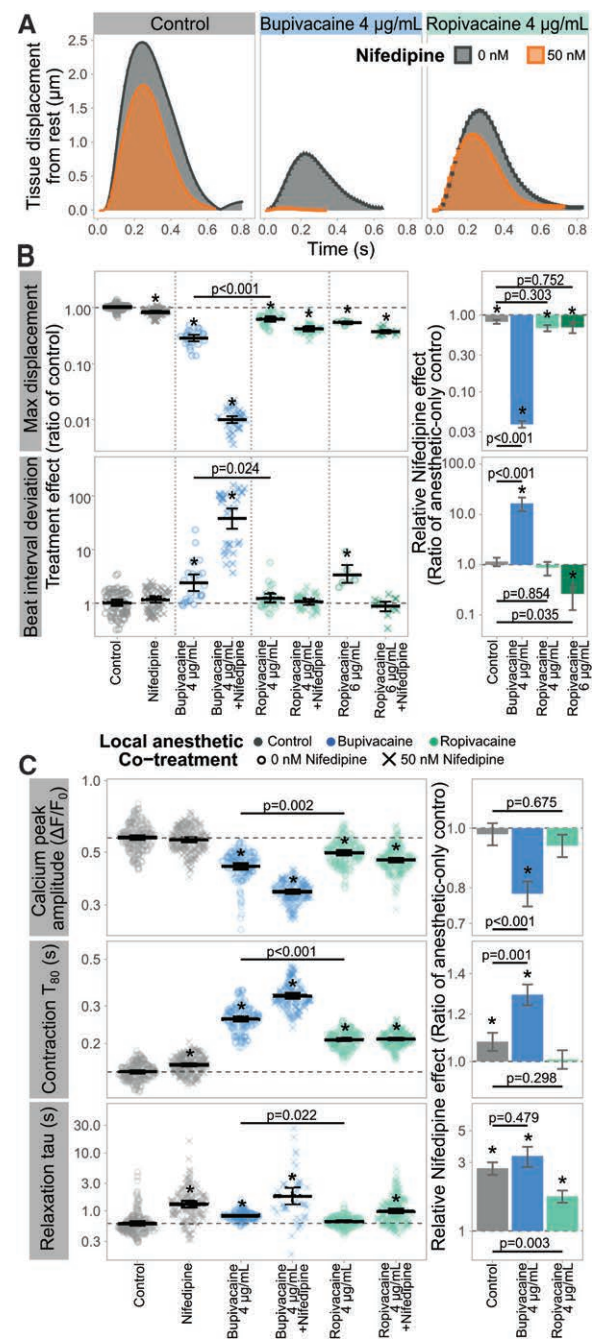


Fig. 5. Nifedipine exacerbates bupivacaine toxicity in induced pluripotent stem cell-derived cardiomyocyte tissues. Tissues were treated with 2, 4, or $6 \mu\text{g/ml}$ bupivacaine or ropivacaine after baseline recordings. Where indicated, a subset of tissues was concurrently treated with 50 nM nifedipine. (A) Representative brightfield tissue motion profiles illustrating changes to contractile function (tissue displacement) with anesthetic and nifedipine treatment. Nifedipine profoundly reduced the contraction of bupivacaine-treated tissues, but marginally (*continued*)

Fig. 5. (continued) changed ropivacaine-treated samples, similar to nifedipine-only controls. (B) Quantification of changes to tissue contractility (maximum tissue displacement) and beating irregularity (beat interval deviation) show that nifedipine exacerbated bupivacaine, but not ropivacaine, effects to both metrics (relative effect shown in the right). $n = 4$ tissues per group with 6 measurements per tissue for control, nifedipine, and 4 $\mu\text{g/ml}$ anesthetic groups; three tissues with 2 to 4 measurements per tissue otherwise. Parameters for the 6 $\mu\text{g/ml}$ bupivacaine + nifedipine group were unquantifiable due to complete beating arrest (Supplemental Video 1, <http://links.lww.com/ALN/C937>). Due to this beating cessation, and because nifedipine effects did not differ at 2 $\mu\text{g/ml}$ anesthetic (Supplemental Figure S9, <http://links.lww.com/ALN/C936>), intracellular calcium dynamics were evaluated for the 4 $\mu\text{g/ml}$ groups. (C) Quantified effects (as in fig. 4A) show nifedipine-mediated perturbation of contraction-phase calcium in bupivacaine, but not ropivacaine-treated tissues. $n = 4$ tissues per group with 10 to 36 measurements per tissue for C. The differential effects of nifedipine were supported by anesthetic and cotreatment interaction $P < 0.001$ for all metrics, except $P = 0.004$ for calcium amplitude. Data are mean and 95% bootstrap CI at 5 h after treatment. Bars are mixed-effects model estimates and standard error for nifedipine effect compared to each respective anesthetic-only control. * $P < 0.05$ treatment versus control; all comparisons determined using *post hoc* multiplicity-adjusted Welch's *t*-tests of model estimates. Data for 2 $\mu\text{g/ml}$ is presented in Supplemental Figure S9 (<http://links.lww.com/ALN/C936>).

and ECG monitoring until asystole (death). To evaluate the effects of calcium supplementation, intravenous calcium chloride pretreatment (10 mg/kg) was compared to saline pretreatment control for each anesthetic (fig. 6 and Supplemental Figures S6 and S7, <http://links.lww.com/ALN/C936>). The pretreatment model was chosen instead of cotreatment to promote delivery of a constant amount of calcium to each animal, despite any differences in survival.

Ropivacaine-treated animals survived longer than bupivacaine (time to asystole— 23.1 ± 5.0 min for bupivacaine and 52.1 ± 5.3 min for ropivacaine, corresponding to 46 ± 10 mg/kg bupivacaine and 104 ± 11 mg/kg ropivacaine, $P = 0.002$). Calcium pretreatment prolonged survival in bupivacaine-treated animals ($+8.3 \pm 2.3$ min, $P = 0.007$), but reduced survival with ropivacaine (-13.8 ± 3.4 min, $P = 0.003$; fig. 6A and Supplemental Figure S6A, <http://links.lww.com/ALN/C936>). At midpoint survival time (*i.e.*, half-time to asystole, corresponding to 27 ± 2 mg/kg bupivacaine infused), we observed higher diastolic pressure ($P = 0.012$) and heart rate ($P < 0.001$) in calcium pretreated bupivacaine animals, signifying partial mitigation of bupivacaine cardiotoxicity (fig. 6B and Supplemental Figure S6, <http://links.lww.com/ALN/C936>). However, calcium pretreatment showed no significant effects on blood pressure or heart rate in ropivacaine animals ($P > 0.9$). Interestingly, calcium supplementation paradoxically decreased terminal serum ionized calcium concentration in bupivacaine-treated animals but had the expected effect of increasing calcium in ropivacaine-treated animals (fig. 6C and Supplemental Figure S7, <http://links.lww.com/ALN/C936>).

This difference may be a manifestation of the previously noted local anesthetic tissue accumulation (up to nine times the arterial value in *ex vivo* guinea pig hearts),³⁷ where the dysregulation of calcium dynamics specifically by elevated bupivacaine may differentially affect the tight regulation of intra- and extracellular calcium concentrations. Furthermore, terminal ion changes may be affected by differences in timing from pretreatment to asystole between animals. Changes in serum glucose were normalized by calcium supplementation between the two anesthetics (Supplemental Figure S7B, <http://links.lww.com/ALN/C936>). In contrast to serum calcium concentrations, we observed no significant differences between groups in changes to serum sodium and potassium, which emphasizes effects on calcium flux in differentiating bupivacaine and ropivacaine toxicity (fig. 6C and Supplemental Figure S7, <http://links.lww.com/ALN/C936>).

Similar to survival data, arrhythmias, marked by early or delayed afterdepolarizations and irregular RR intervals in the ECG (Supplemental Figure S6D, <http://links.lww.com/ALN/C936>), were observed earlier in bupivacaine animals (time to first arrhythmia at 10.6 ± 5.1 min for bupivacaine *vs.* 45.1 ± 5.2 min for ropivacaine, $P < 0.001$). Calcium supplementation prolonged the time to first arrhythmia in bupivacaine-treated animals ($+6.8 \pm 2.4$ min, $P = 0.026$), but reduced it with ropivacaine (-12.0 ± 2.9 min, $P = 0.002$; fig. 6D). Poincaré visualization of beat-to-beat (RR) intervals mirrors these effects—RR intervals deviate more in bupivacaine *versus* ropivacaine rats, indicating more irregular beating (fig. 6E). Calcium pretreatment reduced this spread in bupivacaine animals, indicating improved beating regularity, but markedly increased RR interval spread in ropivacaine animals. These findings illustrate the mitigation of bupivacaine-induced, but exacerbation of ropivacaine-induced, contractile dysfunction and arrhythmias by calcium supplementation, and support our stem cell-derived cardiomyocyte tissue findings.

L-Type Calcium Channel Blockade Selectively Worsens Bupivacaine Toxicity

Previous reports indicated that L-type calcium channel inhibition can exacerbate bupivacaine cardiotoxicity in preclinical models.^{38,39} Given our findings that bupivacaine adversely alters intracellular calcium dynamics, we sought to determine if bupivacaine effects are altered by calcium channel blockers by quantifying the effects of nifedipine on anesthetic-induced contractile depression and calcium dynamics in stem cell-derived cardiomyocyte tissues (fig. 5 and Supplemental Figures S8 to S10, <http://links.lww.com/ALN/C936>).

We found no significant adverse effects of nifedipine cotreatment (50 nM) with either anesthetic at the subtoxic anesthetic dose (2 $\mu\text{g/ml}$) on tissue contractility or beating rhythm (Supplemental Figure S9B, <http://links.lww.com/ALN/C936>). However, with higher doses of bupivacaine, the addition of nifedipine drastically reduced tissue displacement (to $5 \pm 1\%$ of 4 $\mu\text{g/ml}$ bupivacaine-only

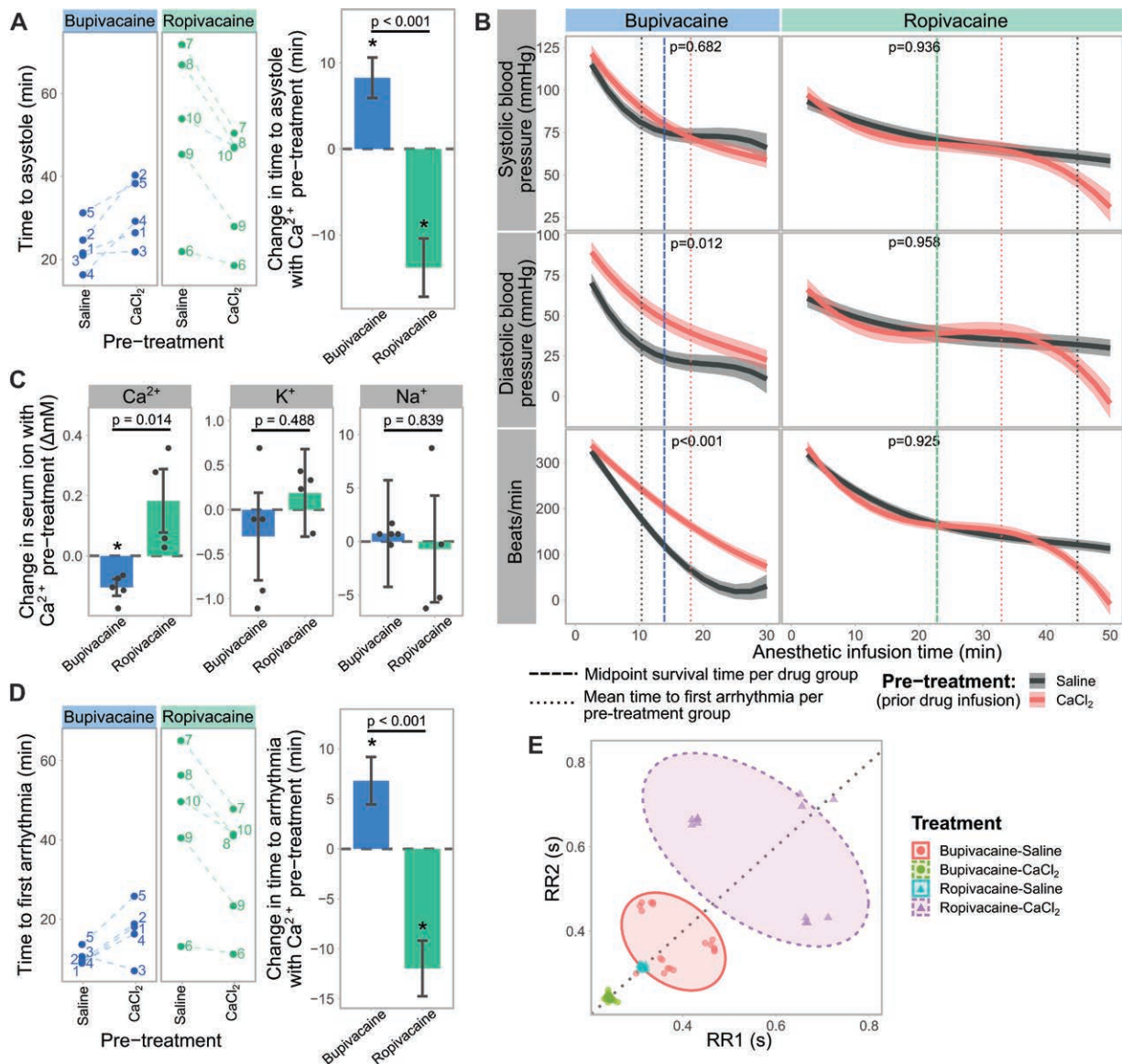


Fig. 6. Calcium pretreatment attenuates bupivacaine toxicity in an *in vivo* rat model. Animal pretreatment (equivalent volume of saline or 10 mg/kg CaCl_2) was intravenously infused for 5 min, after which only bupivacaine or ropivacaine were infused ($2 \text{ mg} \cdot \text{kg}^{-1} \cdot \text{min}^{-1}$) until asystole (death). $n = 5$ animals per group. (A and D) Time to first arrhythmia and time to asystole shown for each animal paired by cage, indicated by matched numbers and dashes (left). Calcium prolonged (improved) both metrics with bupivacaine but reduced (worsened) the times with ropivacaine. $*P < 0.05$ for calcium chloride pretreatment compared to saline controls (*post hoc* Welch's *t* test of mixed-effects model estimates). (B) Time course analysis of anesthetic infusion and calcium supplementation on hemodynamic parameters, showing mitigation of bupivacaine adverse effects on diastolic blood pressure and heart rate with calcium pretreatment. Calcium had no effect on ropivacaine-induced hemodynamic changes. $n = 5$ animals per group; 9 to 16 measurements per animal; *P* values shown for calcium chloride versus saline groups at midpoint survival time per anesthetic. (C) Relative effect of calcium pretreatment on change in blood ion concentrations (from preinfusion to postmortem) highlights differences in calcium flux between bupivacaine and ropivacaine, compared to sodium and potassium (no significant changes). (E) Poincaré plot of adjacent beat-to-beat intervals (RR1 and RR2) at midpoint survival time per anesthetic group, showing beat interval deviation between treatment groups as 90% confidence ellipses around the points. Higher point dispersion indicates increased beating irregularity. Calcium mitigated bupivacaine-related beating irregularity but exacerbated the adverse effect of ropivacaine.

tissues, $P < 0.001$), and increased beat interval deviation (14.5 ± 5.2 -fold of $4 \mu\text{g}/\text{ml}$ bupivacaine-only tissues, $P < 0.001$), indicative of impaired contractility and increased

arrhythmogenesis (fig. 5, A and B). At $6 \mu\text{g}/\text{ml}$ bupivacaine, nifedipine cotreatment completely arrested tissue beating (Supplemental Video 1, <http://links.lww.com/ALN/C937>).

At 4 $\mu\text{g}/\text{ml}$, nifedipine cotreatment perturbed sarcoplasmic calcium flux during contraction, decreasing peak calcium wave amplitude (to $78 \pm 4\%$ of bupivacaine-only tissues, $P < 0.001$; fig. 5C). Even at toxic anesthetic concentrations, nifedipine did not produce a measurable adverse effect on tissue contractility or intracellular calcium dynamics in ropivacaine-treated tissues (fig. 5, Supplemental Video 1, <http://links.lww.com/ALN/C937>). Interestingly, nifedipine cotreatment actually reduced beating irregularity, indicating partial mitigation of ropivacaine-induced arrhythmias at 6 $\mu\text{g}/\text{ml}$ anesthetic ($P = 0.035$, fig. 5B). Furthermore, we observed an improved calcium relaxation rate constant tau in ropivacaine–nifedipine tissues, compared to nifedipine-only controls, signifying improved sarcoplasmic calcium reuptake due to the ropivacaine–nifedipine interaction ($P = 0.003$, fig. 5C).

Overall, nifedipine potentiated bupivacaine-mediated contractile depression, beating irregularity, and sarcolemmal calcium dysfunction, while showing no adverse (and some beneficial) effects with ropivacaine. Our findings indicate that L-type calcium channel blockade produces a synergistic effect that exacerbates the adverse changes to cardiomyocyte function induced by toxic bupivacaine concentrations. This relationship does not exist between ropivacaine and nifedipine, and calcium blockade may partially mitigate ropivacaine toxicity. The divergent effect of calcium blockers between the two anesthetics further supports the role of calcium flux as key to their markedly different cardiotoxicities.

Discussion

Pharmaceuticals exhibit unexpected postmarket cardiotoxicity, partially due to a deficit of preclinical models that reliably predict drug activity in the human heart.^{14,16} Testing on induced pluripotent stem cell–derived cardiomyocytes could improve drug safety by providing a native human cellular context, as illustrated by previous successful evaluations of ion channel modulators, arrhythmogens, and inotropes, showing parity to known *in vivo* effects.^{14–16,40} Supporting stem cell–derived cardiomyocyte model pertinence, we found no adverse effect of local anesthetics tested less than 2 $\mu\text{g}/\text{ml}$, agreeing with *in vivo* data.^{27,29} Above the toxicity threshold, at concentrations systemically achievable during routine anesthetic use,^{27,28,30,31} all drugs illustrated signs of toxicity, as expected given their known $\text{Na}_v1.5$ cardiac sodium channel inhibition. However, resulting from distinct cellular physiology changes, we observed different magnitudes of toxicity between bupivacaine and ropivacaine, consistent with clinically evident cardiotoxicity differences between these two drugs.

Conforming to the canonical mechanism of cardiotoxicity, we observed a markedly reduced sodium current spike amplitude with all drugs, although bupivacaine exhibited greater inhibition. Published studies showed small differences between anesthetic blockade of human $\text{Na}_v1.5$ in the clinically relevant inactive channel form (bupivacaine IC_{50} $2.2 \pm 0.2 \mu\text{M}$ vs. ropivacaine $2.7 \pm 0.3 \mu\text{M}$), concluding that

other mechanisms are likely.⁹ Moreover, such isolated channel studies lack the native cardiac proteome context, where channel modulation by regulatory proteins and other nearby channels can alter drug effects.^{22,41} In isolated canine cardiomyocytes, used for their proposed electrophysiologic similarity to human cardiomyocytes, sodium current inhibition was the dominant effect observed for bupivacaine and ropivacaine.⁴² At concentrations similar to our study, bupivacaine induced a 2-fold stronger inhibition than ropivacaine, consistent with our data. Interestingly, the authors noted differences in the ropivacaine ion current inhibition profiles between artificial patch clamp and physiologic cardiomyocyte states, reiterating the importance of studying anesthetic toxicity in a native, contractile cellular context.

In contractile cardiomyocytes, the regulation of sodium and calcium flux is closely tied.^{22,41} In addition to $\text{Na}_v1.5$ blockade, bupivacaine was previously observed to inhibit calcium currents, intracellular calcium dynamics, and sarcolemmal proteins (ryanodine receptor and sarcoendoplasmic reticulum calcium ATPase *via* calcium reuptake) more than ropivacaine in mammalian muscle preparations, but at concentrations significantly higher (more than 2,500 $\mu\text{g}/\text{ml}$) than the clinically relevant range.^{43,44} Closer to expected serum concentration (3 $\mu\text{g}/\text{ml}$), bupivacaine partially inhibited slow L-type calcium currents, but direct comparisons to ropivacaine were not investigated.^{11,36} Just above the toxicity threshold (at 3, 6 $\mu\text{g}/\text{ml}$), we noted that bupivacaine prolonged early (in the contractile cycle) cellular field potentials, primarily mediated by L-type calcium channels and ryanodine receptor sarcoplasmic calcium efflux, whereas ropivacaine or levobupivacaine showed negligible effects (fig. 2). Additionally, bupivacaine more strongly inhibited sarcoplasmic calcium release during contraction, and subsequent reuptake during relaxation, at both 4 and 6 $\mu\text{g}/\text{ml}$ (figs. 4 and 5). This indicates inhibition of the sarcoendoplasmic reticulum calcium ATPase and the sodium–calcium exchanger (which help remove cytosolic calcium during relaxation).²² Thus, our data support calcium dynamics dysregulation being a key bupivacaine cardiotoxicity mediator. However, differences in binding modes at specific intracellular targets relevant to calcium flux remain to be elucidated. In rats, bupivacaine was observed to bind the dihydropyridine neuronal L-type calcium channel site 2-fold more potently than *R*- and *S*-ropivacaine.⁴⁵ Such studies in human contractile cardiomyocytes, including *R*-ropivacaine and dextropropivacaine, can further define molecular cardiotoxicity mechanistic differences, along with stereospecific effects, which we did not investigate. This would enhance our understanding of structure–activity relationships to therapeutic and cardiotoxic anesthetic effects, helping inform future drug design and reduce off-target toxicity.

Calcium modulation is fundamental to cardiomyocyte contractility and beating rhythm. Excess calcium (endogenous or exogenous) can lead to toxicity and arrhythmogenesis.²² Moderate calcium supplementation can be used for inotropic support during cardiac resuscitation and is particularly effective

with baseline hypocalcemia.³⁵ We found that calcium supplementation mitigated bupivacaine cardiotoxic effects but had no effect (or exacerbated) ropivacaine functional decline *in vitro* (figs. 3 and 4). We observed similar effects of calcium supplementation in rats (fig. 6), underscoring the importance of calcium flux in cardiotoxicity mechanisms of different anesthetics. Previously, calcium supplementation reduced bupivacaine arrhythmias potentiated by high potassium buffer in isolated rat cardiomyocytes⁴⁶; however, calcium effects on anesthetic alone were not addressed. We found that intravenous calcium pretreatment delayed time to first arrhythmia and asystole, and mitigated diastolic blood pressure and heart rate decline in bupivacaine-treated animals. Ropivacaine effects were opposing, where exogenous calcium reduced survival and promoted arrhythmias. Thus, calcium could be used to attenuate bupivacaine, but not ropivacaine effects, illustrating how calcium preconditions may affect anesthetic-specific cardiotoxicity risk.

In mammalian ventricular muscle, bupivacaine was noted to lower myofilament calcium sensitivity more effectively than ropivacaine (*i.e.*, more intracellular calcium required to generate equal force).^{47,48} We observed, similar to other studies, that bupivacaine can inhibit sarcoplasmic calcium release (lower peak calcium wave amplitude). The combination of lower myofilament calcium sensitivity and reduced calcium cycling suggests that supplemental calcium might be beneficial in mitigating bupivacaine-induced contractile depression. This notion is supported by our *in vitro* and *in vivo* findings. In a mouse study of neuronal pain-sensing, pharmacologic calcium channel activation reduced bupivacaine analgesia, implying that increased intracellular calcium flux may interfere with the inhibitory channel effects of bupivacaine.⁴⁹ This finding mirrors the protective supplemental calcium effect on bupivacaine cardiotoxicity that we observed.

Calcium dysregulation represents a unique adverse bupivacaine effect, without parallel findings for ropivacaine at the concentrations studied. The divergent calcium supplementation effect on anesthetic toxicity highlights the need for anesthetic- and context-specific risk evaluation. Studies in mice indicate that calcium channel inhibitors can exacerbate bupivacaine lethality and enhance contractile depression in guinea pigs and dogs.^{38,39} Specifically, experiments in guinea pig myocardium suggest that at drug doses similar to our study, bupivacaine and nifedipine interactions do not directly involve $\text{Na}_v1.5$ inhibition, but are due to synergistic block of L-type calcium channels.³⁹ Consistent with this, we did not observe any effects on calcium-related field potentials or intracellular calcium flux by either anesthetic, or any adverse nifedipine interactions, at subtoxic anesthetic doses. However, above the toxicity threshold, bupivacaine synergistically interacted with nifedipine to further depress contractility and increase arrhythmias. Ropivacaine was not previously compared to bupivacaine in this context. Our findings contrast bupivacaine, whereas nifedipine did not potentiate ropivacaine cardiotoxicity, instead improving

sarcoplasmic calcium reuptake and beating regularity. The divergent nifedipine-anesthetic interaction suggests that calcium preconditions may affect toxicity risk and reiterates the importance of calcium flux in anesthetic cardiotoxicity.

Although stem cell-derived cardiomyocytes offer a sustainable human cardiomyocyte source, with demonstrated utility in disease modeling and drug development,^{14,16,40} they initially exhibit a neonatal phenotype. Strategies exist to mature the cells (*e.g.*, see Materials and Methods), but components of metabolism, sarcomere structure, and ion flux may lie at intermediate maturation states relative to adult human myocardium.^{21,24} Other limitations include the lack of hemodynamic effects and coronary flow in our tissue model, where anesthetic concentrations remain static during treatment. The 5-h incubation may not represent immediate clinical cardiotoxicity; however, the timing is comparable to amide anesthetic block durations and elimination half-lives (*i.e.*, slow perivascular absorption *vs.* acute toxicity). There may be discrepancies between media/serum and effect site (tissue) concentrations due to differences in biologic uptake,³⁷ and 11-fold higher liposolubility of bupivacaine and levobupivacaine than ropivacaine.⁸ We did not adjust concentrations based on ropivacaine and bupivacaine lipid solubilities or anesthetic potencies. Due to ethical reasons, quantifying human therapeutic potency is challenging. This results in varying therapeutic potency differences reported for anesthetics that depend on nerve block type (*e.g.*, between 2-fold higher for bupivacaine than ropivacaine in epidural labor analgesia, to equipotency in femoral nerve block).⁸ This issue is further compounded by differences in drug liposolubility and potential tissue accumulation, and between myocardial and neuronal diffusion barriers.^{8,37,50} However, overall trends indicate ~0.7:0.9:1.0 relative ratio for ropivacaine:levobupivacaine:bupivacaine therapeutic potency,^{5,8,51} suggesting similarity to cardiotoxicity differences and similar toxicity risk at equipotent concentrations. Interestingly, we observed levobupivacaine effects comparable to ropivacaine, in particular, both lacked effects on calcium-related repolarization. Furthermore, nifedipine did not negatively interact with 6 $\mu\text{g}/\text{ml}$ ropivacaine but was detrimental with 4 $\mu\text{g}/\text{ml}$ bupivacaine (near equipotent concentrations). These findings support the unique bupivacaine effects on calcium dynamics. However, as we focused on select clinically relevant concentrations, additional concentrations can help more completely quantify the relationship to therapeutic anesthetic potency differences. Because clinical cardiotoxicity is difficult to predict, our calcium prophylaxis rat model is likely impractical. Moreover, we studied female rats due to animal availability; thus, we did not capture possible sex-specific differences.

Conclusions

We found that bupivacaine adversely altered cardiomyocyte calcium dynamics in a functional human-derived tissue model (fig. 7). The same effect was not observed with ropivacaine, where toxicity risk is lower. Calcium

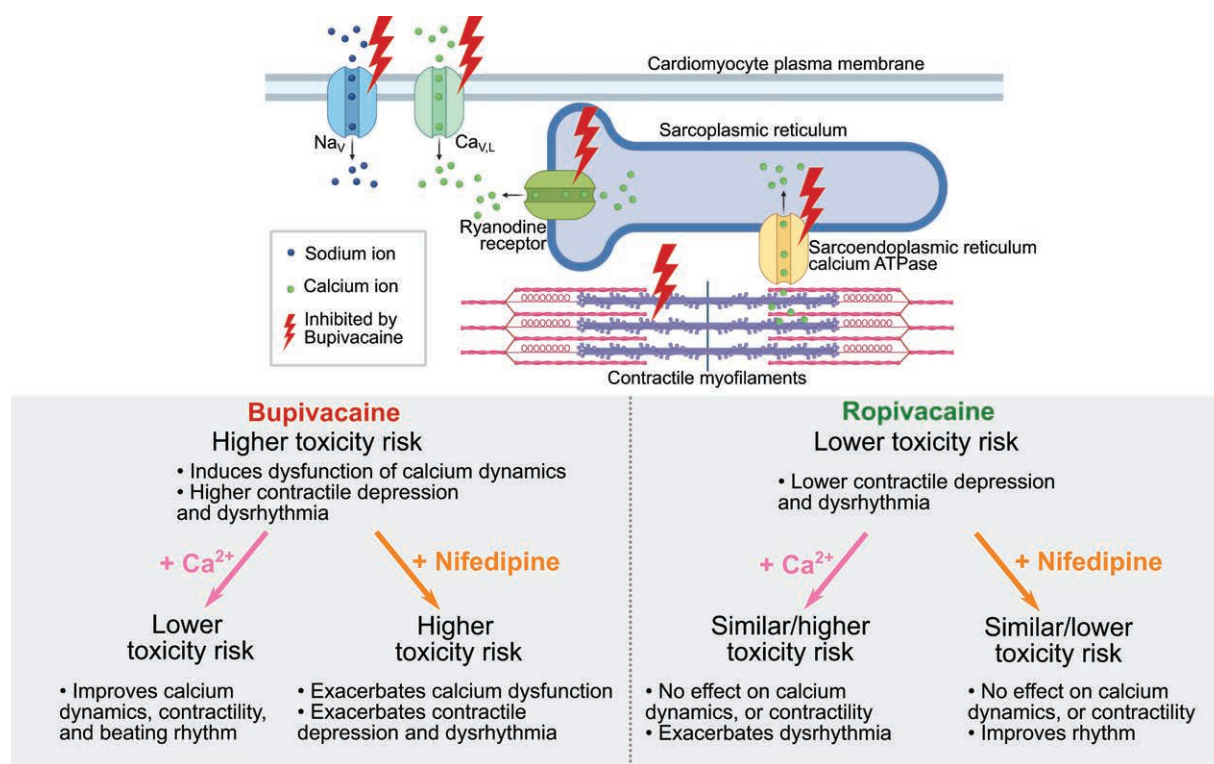


Fig. 7. Summary of the distinct effects of local anesthetics on cardiomyocyte calcium dynamics. At clinically relevant supratoxic local anesthetic concentrations (3 to 6 $\mu\text{g}/\text{ml}$), racemic bupivacaine more strongly inhibited the $\text{Na}_v1.5$ cardiac sodium channel, and all tested phases of intracellular calcium dynamics, than ropivacaine. These ion effects worsened the contractile depression and dysrhythmia caused by bupivacaine. Exogenous calcium supplementation ($+\text{Ca}^{2+}$) improved contractility and beating rhythm with bupivacaine, but exacerbated dysrhythmia with ropivacaine. Conversely, calcium blockade via the L-type calcium channel blocker nifedipine exacerbated bupivacaine contractile depression and dysrhythmia, but improved beating rhythm with ropivacaine. Therefore, our work suggests that anesthetic-specific cardiotoxicity risks may be influenced by calcium-dependent toxicity contexts (e.g., hypo- or hypercalcemia).

supplementation prevented bupivacaine, but exacerbated ropivacaine, cardiotoxicity *in vitro* and in rats. Nifedipine coadministration worsened bupivacaine, but not ropivacaine, cardiotoxicity at the clinically relevant concentrations studied, suggesting that bupivacaine toxicity could be potentiated by adverse interactions with calcium channel blockers. Our data highlight the distinct role of calcium dynamics in the higher cardiotoxicity risk of bupivacaine and suggest that calcium modulation may mitigate bupivacaine detrimental effects. Our approach provides a model to understand the broader issue of postmarket cardiotoxicity demonstrated by other drugs, correlating *in vitro* testing to adverse *in vivo* activity.

Acknowledgments

The authors thank Kyu Kim, M.Sc. (University of Toronto, Toronto, Ontario, Canada) and Boris Hinz, Ph.D. (University of Toronto, Toronto, Ontario, Canada) for providing the 5 kPa silicone microplates used in *in vitro* studies. The authors thank the members of the Department of Anesthesia and Pain Medicine at the Hospital for Sick Children (Toronto,

Ontario, Canada) for the protection of research time for the study investigators. Dr. Maynes would also like to thank the Wasser Family and SickKids Foundation as the holder of the Wasser Chair in Anesthesia and Pain Medicine.

Research Support

The authors acknowledge the financial support from the Canadian Institute for Health Research (CIHR; Ottawa, Ontario, Canada) and the Natural Sciences and Engineering Research Council of Canada (NSERC; Ottawa, Ontario, Canada).

Competing Interests

The authors declare no conflicts of interest.

Correspondence

Address correspondence to Dr. Maynes, Hospital for Sick Children, 555 University Ave, Toronto, Canada M5G 1X8. jason.maynes@sickkids.ca. This article may be accessed for personal use at no charge through the Journal Web site, www.anesthesiology.org.

Supplemental Digital Content

Supplementary data, <http://links.lww.com/ALN/C936>
Supplementary video, <http://links.lww.com/ALN/C937>

References

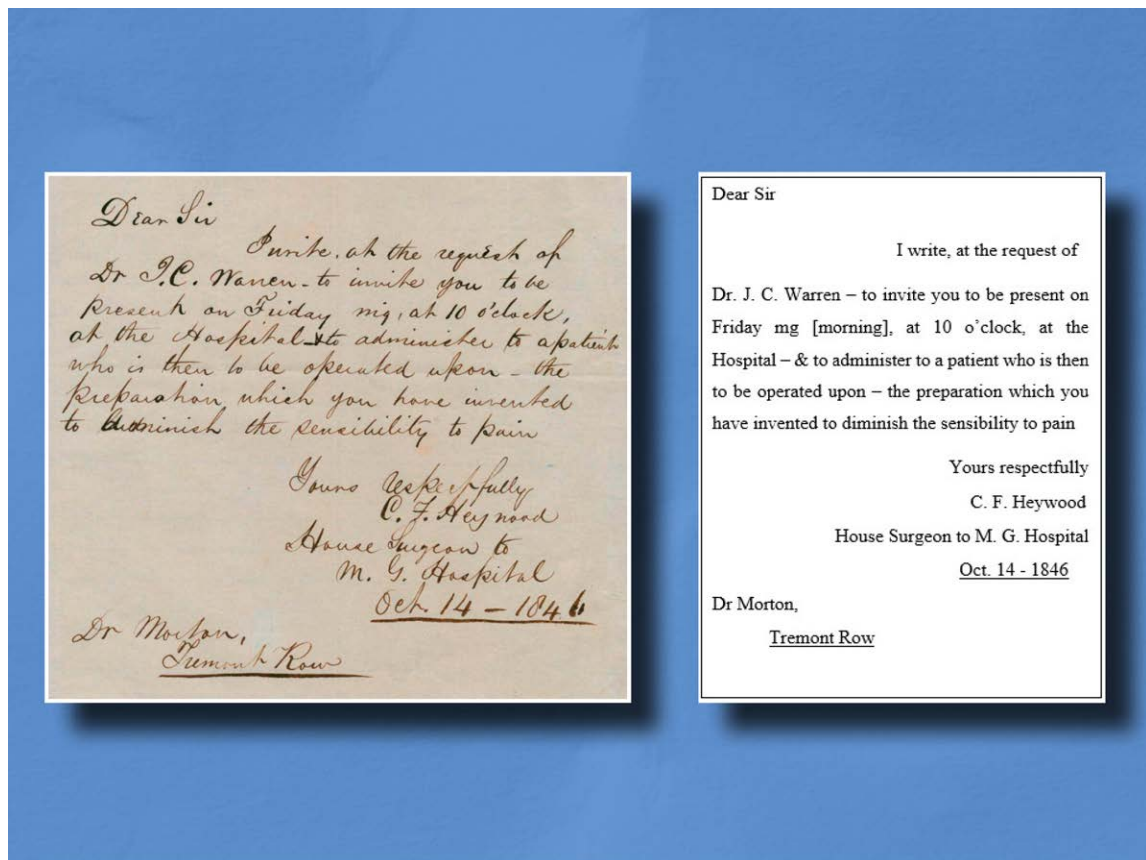
1. Neal JM, Barrington MJ, Fettiplace MR, Gitman M, Mementsoudis SG, Mörwald EE, Rubin DS, Weinberg G: The third American Society of Regional Anesthesia and Pain Medicine Practice Advisory on Local Anesthetic Systemic Toxicity: executive summary 2017. *Reg Anesth Pain Med* 2018; 43:113–23
2. Gitman M, Barrington MJ: Local anesthetic systemic toxicity: A review of recent case reports and registries. *Reg Anesth Pain Med* 2018; 43:124–30
3. Otero PE, Fuensalida SE, Russo PC, Verdier N, Blanco C, Portela DA: Mechanism of action of the erector spinae plane block: Distribution of dye in a porcine model. *Reg Anesth Pain Med* 2020; 45:198–203
4. De Cassai A, Bonanno C, Padriani R, Geraldini F, Boscolo A, Navalesi P, Munari M: Pharmacokinetics of lidocaine after bilateral ESP block. *Reg Anesth Pain Med* 2021; 46:86–9
5. Gitman M, Fettiplace MR, Weinberg GL, Neal JM, Barrington MJ: Local anesthetic systemic toxicity: A narrative literature review and clinical update on prevention, diagnosis, and management. *Plast Reconstr Surg* 2019; 144:783–95
6. Groban L, Dolinski SY: Differences in cardiac toxicity among ropivacaine, levobupivacaine, bupivacaine, and lidocaine. *Tech Reg Anesth Pain Manag* 2001; 5:48–55
7. Butterworth JF IV: Models and mechanisms of local anesthetic cardiac toxicity: a review. *Reg Anesth Pain Med* 2010; 35:167–76
8. Casati A, Putzu M: Bupivacaine, levobupivacaine and ropivacaine: are they clinically different? *Best Pract Res Clin Anaesthesiol* 2005; 19:247–68
9. Schwoerer AP, Scheel H, Friederich P: A comparative analysis of bupivacaine and ropivacaine effects on human cardiac SCN5A channels. *Anesth Analg* 2015; 120:1226–34
10. El-Boghdady K, Pawa A, Chin KJ: Local anesthetic systemic toxicity: Current perspectives. *Local Reg Anesth* 2018; 11:35–44
11. Coyle DE, Sperelakis N: Bupivacaine and lidocaine blockade of calcium-mediated slow action potentials in guinea pig ventricular muscle. *J Pharmacol Exp Ther* 1987; 242:1001–5
12. Butterworth J, James RL, Grimes J: Structure-affinity relationships and stereospecificity of several homologous series of local anesthetics for the beta2-adrenergic receptor. *Anesth Analg* 1997; 85:336–42
13. Weinberg GL, Palmer JW, VadeBoncouer TR, Zuechner MB, Edelman G, Hoppel CL: Bupivacaine inhibits acylcarnitine exchange in cardiac mitochondria. *ANESTHESIOLOGY* 2000; 92:523–8
14. Pang L, Sager P, Yang X, Shi H, Sannaajust F, Brock M, Wu JC, Abi-Gerges N, Lyn-Cook B, Berridge BR, Stockbridge N: Workshop report: FDA workshop on improving cardiotoxicity assessment with human-relevant platforms. *Circ Res* 2019; 125:855–67
15. Wang L, Dou W, Malhi M, Zhu M, Liu H, Plakhotnik J, Xu Z, Zhao Q, Chen J, Chen S, Hamilton R, Simmons CA, Maynes JT, Sun Y: Microdevice platform for continuous measurement of contractility, beating rate, and beating rhythm of human-induced pluripotent stem cell-cardiomyocytes inside a controlled incubator environment. *ACS Appl Mater Interfaces* 2018; 10:21173–83
16. Bruyneel AA, McKeithan WL, Feyen DA, Mercola M: Will iPSC-cardiomyocytes revolutionize the discovery of drugs for heart disease? *Curr Opin Pharmacol* 2018; 42:55–61
17. Kennedy A, Finlay DD, Guldenring D, Bond RR, Moran K, McLaughlin J: Automated detection of atrial fibrillation using R-R intervals and multivariate-based classification. *J Electrocardiol* 2016; 49:871–6
18. Monfredi O, Lyashkov AE, Johnsen A-B, Inada S, Schneider H, Wang R, Nirmalan M, Wisloff U, Maltsev VA, Lakatta EG, Zhang H, Boyett MR: Biophysical characterization of the underappreciated and important relationship between heart rate variability and heart rate. *Hypertension* 2014; 64:1334–43
19. Li CX, Talele NP, Boo S, Koehler A, Knee-Walden E, Balestrini JL, Speight P, Kapus A, Hinz B: MicroRNA-21 preserves the fibrotic mechanical memory of mesenchymal stem cells. *Nat Mater* 2017; 16:379–89
20. Engler AJ, Carag-Krieger C, Johnson CP, Raab M, Tang HY, Speicher DW, Sanger JW, Sanger JM, Discher DE: Embryonic cardiomyocytes beat best on a matrix with heart-like elasticity: scar-like rigidity inhibits beating. *J Cell Sci* 2008; 121(Pt 22):3794–802
21. Guo Y, Pu WT: Cardiomyocyte maturation: New phase in development. *Circ Res* 2020; 126:1086–106
22. Fearnley CJ, Roderick HL, Bootman MD: Calcium signaling in cardiac myocytes. *Cold Spring Harb Perspect Biol* 2011; 3:a004242
23. Maddah M, Heidmann JD, Mandegar MA, Walker CD, Bolouki S, Conklin BR, Loewke KE: A non-invasive platform for functional characterization of stem-cell-derived cardiomyocytes with applications in cardiotoxicity testing. *Stem Cell Reports* 2015; 4:621–31
24. Argenziano M, Lambers E, Hong L, Sridhar A, Zhang M, Chalazan B, Menon A, Savio-Galimberti E, Wu JC, Rehman J, Darbar D: Electrophysiologic characterization of calcium handling in human induced pluripotent stem cell-derived atrial cardiomyocytes. *Stem Cell Reports* 2018; 10:1867–78
25. Lu HR, Whittaker R, Price JH, Vega R, Pfeiffer ER, Cerignoli F, Towart R, Gallacher DJ: High throughput

- measurement of Ca^{++} dynamics in human stem cell-derived cardiomyocytes by kinetic image cytometry: A cardiac risk assessment characterization using a large panel of cardioactive and inactive compounds. *Toxicol Sci* 2015; 148:503–16
26. Wong GK, Crawford MW: Carnitine deficiency increases susceptibility to bupivacaine-induced cardiotoxicity in rats. *ANESTHESIOLOGY* 2011; 114:1417–24
 27. Trabelsi B, Charfi R, Bennasr L, Marzouk SB, Eljebari H, Jebabli N, Sassi MB, Trabelsi S, Maghrebi H: Pharmacokinetics of bupivacaine after bilateral ultrasound-guided transversus abdominis plane block following cesarean delivery under spinal anesthesia. *Int J Obstet Anesth* 2017; 32:17–20
 28. Chazalon P, Tourtier JP, Villevielle T, Giraud D, Saïssy JM, Mion G, Benhamou D: Ropivacaine-induced cardiac arrest after peripheral nerve block: successful resuscitation. *ANESTHESIOLOGY* 2003; 99:1449–51
 29. Rahiri J, Tuhoe J, Svirskis D, Lightfoot NJ, Lirk PB, Hill AG: Systematic review of the systemic concentrations of local anaesthetic after transversus abdominis plane block and rectus sheath block. *Br J Anaesth* 2017; 118:517–26
 30. Berrisford RG, Sabanathan S, Mearns AJ, Clarke BJ, Hamdi A: Plasma concentrations of bupivacaine and its enantiomers during continuous extrapleural intercostal nerve block. *Br J Anaesth* 1993; 70:201–4
 31. Griffiths JD, Le NV, Grant S, Bjorksten A, Hebbard P, Royse C: Symptomatic local anaesthetic toxicity and plasma ropivacaine concentrations after transversus abdominis plane block for Caesarean section. *Br J Anaesth* 2013; 110:996–1000
 32. Zhang X, Guo L, Zeng H, White SL, Furniss M, Balasubramanian B, Lis E, Lagrutta A, Sannajust F, Zhao LL, Xi B, Wang X, Davis M, Abassi YA: Multi-parametric assessment of cardiomyocyte excitation-contraction coupling using impedance and field potential recording: A tool for cardiac safety assessment. *J Pharmacol Toxicol Methods* 2016; 81:201–16
 33. Tertoolen LGJ, Braam SR, van Meer BJ, Passier R, Mummery CL: Interpretation of field potentials measured on a multi electrode array in pharmacological toxicity screening on primary and human pluripotent stem cell-derived cardiomyocytes. *Biochem Biophys Res Commun* 2018; 497:1135–41
 34. Kussauer S, David R, Lemcke H: hiPSCs derived cardiac cells for drug and toxicity screening and disease modeling: What micro-electrode-array analyses can tell us. *Cells* 2019; 8:E1331
 35. Redman J, Worthley LI: Antiarrhythmic and haemodynamic effects of the commonly used intravenous electrolytes. *Crit Care Resusc* 2001; 3:22–34
 36. Rossner KL, Freese KJ: Bupivacaine inhibition of L-type calcium current in ventricular cardiomyocytes of hamster. *ANESTHESIOLOGY* 1997; 87:926–34
 37. Hiller N, Mirtschink P, Merkel C, Knels L, Oertel R, Christ T, Deussen A, Koch T, Stehr SN: Myocardial accumulation of bupivacaine and ropivacaine is associated with reversible effects on mitochondria and reduced myocardial function. *Anesth Analg* 2013; 116:83–92
 38. Howie MB, Mortimer W, Candler EM, McSweeney TD, Frolicher DA: Does nifedipine enhance the cardiovascular depressive effects of bupivacaine? *Reg Anesth* 1989; 14:19–25
 39. Wulf H, Gödicke J, Herzig S: Functional interaction between local anaesthetics and calcium antagonists in guinea pig myocardium: 2. Electrophysiological studies with bupivacaine and nifedipine. *Br J Anaesth* 1994; 73:364–70
 40. Koci B, Luerman G, Duenbostell A, Kettenhofen R, Bohlen H, Coyle L, Knight B, Ku W, Volberg W, Woska JR, Brown MP: An impedance-based approach using human iPSC-derived cardiomyocytes significantly improves *in vitro* prediction of *in vivo* cardiotoxic liabilities. *Toxicol Appl Pharmacol* 2017; 329:121–7
 41. Kleber AG, Wit AL: The interaction between Na^+ and Ca^{2+} inward currents in cardiac propagation. *Circ Res* 2020; 127:1549–51
 42. Szabó A, Szentandrassy N, Birinyi P, Horváth B, Szabó G, Bányász T, Márton I, Magyar J, Nánási PP: Effects of ropivacaine on action potential configuration and ion currents in isolated canine ventricular cardiomyocytes. *ANESTHESIOLOGY* 2008; 108:693–702
 43. Takahashi S: Local anaesthetic bupivacaine alters function of sarcoplasmic reticulum and sarcolemmal vesicles from rabbit masseter muscle. *Pharmacol Toxicol* 1994; 75:119–28
 44. Komai H, Lokuta AJ: Interaction of bupivacaine and tetracaine with the sarcoplasmic reticulum Ca^{2+} release channel of skeletal and cardiac muscles. *ANESTHESIOLOGY* 1999; 90:835–43
 45. Hirota K, Browne T, Appadu BL, Lambert DG: Do local anaesthetics interact with dihydropyridine binding sites on neuronal L-type Ca^{2+} channels? *Br J Anaesth* 1997; 78:185–8
 46. McCaslin PP, Butterworth J: Bupivacaine suppresses $[\text{Ca}^{2+}]_i$ oscillations in neonatal rat cardiomyocytes with increased extracellular K^+ and is reversed with increased extracellular Mg^{2+} . *Anesth Analg* 2000; 91:82–8
 47. Mio Y, Fukuda N, Kusakari Y, Amaki Y, Tanifuji Y, Kurihara S: Comparative effects of bupivacaine and ropivacaine on intracellular calcium transients and tension in ferret ventricular muscle. *ANESTHESIOLOGY* 2004; 101:888–94
 48. Flenner F, Arlt N, Nasib M, Schobesberger S, Koch T, Ravens U, Friedrich F, Nikolaev V, Christ T, Stehr SN: *In Vitro* negative inotropic effect of low concentrations of bupivacaine relates to diminished Ca^{2+} sensitivity but not to Ca^{2+} handling or β -adrenoceptor signaling. *ANESTHESIOLOGY* 2018; 128:1175–86
 49. Smith FL, Davis RW, Carter R: Influence of voltage-sensitive Ca^{++} channel drugs on bupivacaine infiltration anesthesia in mice. *ANESTHESIOLOGY* 2001; 95:1189–97

50. Tylutki Z, Polak S: Plasma vs heart tissue concentration in humans – Literature data analysis of drugs distribution. *Biopharm Drug Dispos* 2015; 36:337–51
51. Columb M, Gall I: Minimum local analgesic concentration of local anaesthetics. *Contin Educ Anaesth Crit Care Pain* 2010; 10:114–6

ANESTHESIOLOGY REFLECTIONS FROM THE WOOD LIBRARY-MUSEUM

A Prelude to Painless Surgery: Charles F. Heywood's Invitation to W. T. G. Morton



Penned 2 days before surgical etherization's public debut, an invitation (*left*) from house surgeon Charles F. Heywood, M.D. (1823 to 1893), to Boston dentist William T. G. Morton (1819 to 1868) requested that Morton administer his "preparation...to diminish the sensibility to pain" at the Massachusetts General Hospital on October 16, 1846. One of the few extant handwritten documents relating to "Ether Day," the letter is held by the Massachusetts Historical Society, Boston, Massachusetts (W.T. G. Morton papers, call number: Ms. N-567, reproduced with permission). As evidence of his primacy in this discovery, Morton published a different transcript of this letter in the *Statements* volume submitted to the U.S. Congress in 1853, and later in *Trials of a Public Benefactor* (1859), his authorized biography. The advent of painless surgery, a great boon to humanity, would be tarnished almost immediately by the "Ether Controversy." Now a precious historical document, Heywood's letter served as a prologue to "Ether Day" and critical evidence in Morton's ultimately futile claims for financial compensation. (Copyright © the American Society of Anesthesiologists' Wood Library-Museum of Anesthesiology. www.woodlibrarymuseum.org)

Rajesh P. Haridas, M.B.Ch.B., F.A.N.Z.C.A., Sydney, New South Wales, Australia, and Melissa L. Coleman, M.D., Associate Professor, Department of Anesthesiology and Perioperative Medicine, Penn State College of Medicine, Hershey, Pennsylvania.